Available online at www.sciencedirect.com
SCIENCE DIRECT®
Bioorganic & Medicinal Chemistry Letters 15 (2005) 1385–1388
Bioorganic & Medicinal Chemistry Letters

Utilization of a nitrobenzoxadiazole (NBD) fluorophore in the design of a Grb2 SH2 domain-binding peptide mimetic

Zhen-Dan Shi,[a] Rajeshri G. Karki,[a] Shinya Oishi,[a] Karen M. Worthy,[b] Lakshman K. Bindu,[b] Pathirage G. Dharmawardana,[c] Marc C. Nicklaus,[a] Donald P. Bottaro,[c] Robert J. Fisher[b] and Terrence R. Burke, Jr.[a,*]

[a]*Laboratory of Medicinal Chemistry, CCR, NCI, NIH, Frederick, MD 21702, USA*
[b]*Protein Chemistry Laboratory, SAIC-Frederick, Frederick, MD 21702, USA*
[c]*Urology Oncologic Branch, CCR, NCI, NIH, Bethesda, MD 20892, USA*

Received 28 October 2004; revised 4 January 2005; accepted 6 January 2005

Abstract—Fluorescence labeling has become a general technique for studying the intracellular accumulation and localization of exogenously administered materials. Reported herein is a low nanomolar affinity Grb2 SH2 domain-binding antagonist that utilizes the environmentally-sensitive nitrobenzoxadiazole (NBD) fluorophore as a naphthyl replacement. This novel agent should serve as a useful tool to visualize the actions of this class of Grb2 SH2 domain-binding antagonists in whole cell systems.

Phosphotyrosyl (pTyr)-dependent protein–protein interactions mediated by Src homology 2 (SH2) domains provide important connectivity in a variety of pathogenic signaling pathways. In particular, the Grb2 SH2 domain has been implicated in the etiology of several cancers, including erbB-2-dependent breast cancers and c-Met-dependent renal cancers.[1] As one approach toward a new class of anticancer therapeutic, pTyr mimetic-containing Grb2 SH2 domain binding antagonists have been prepared typified by naphthylpropylamide-containing analogues such as **1** and **2** (Fig. 1).[2] Although many of these compounds have exhibited high binding affinity in extracellular assays, in physiological contexts where Grb2 proteins reside in intracellular compartments, persistent concerns exist regarding both the ability of these agents to transit cell membranes and their binding selectivity once inside the cell. Fluorescence labeling has become a general technique for studying the intracellular accumulation and localization of exogenously administered materials.[3] Ideally, use of this approach to study intracellular interactions of Grb2 SH2 domain-binding antagonists of type **2** would require the preparation of highly fluorescent analogues that retain characteristics of the parent structures. The current report details the design and synthesis of nitrobenzoxadiazole (NBD)-containing **3** as a variant of **2** potentially suitable for whole cell Grb2 SH2 domain binding studies.

1. Design and synthesis of target 3

The purpose in preparing a fluorescently-labeled Grb2 SH2 domain-binding inhibitor is to facilitate representative cellular distribution studies of the class of inhibitors typified by parent compound **2**. Therefore, structural similarity of the fluorescent analogue with **2** was desired. Previous studies had delineated the importance of C-terminal 3-(arylbicyclo)propylamido functionality for interaction with a hydrophobic patch formed by residues LeuβD8[4] (Leu111) and PheβE3 (Phe119) of the Grb2 SH2 domain protein.[2a,5] The NBD ring system was chosen as a fluorophore due to its bicyclic nature and its ability to exhibit higher fluorescence when bound to protein surfaces than when free in aqueous media. Incorporation of the NBD unit into the inhibitor structure was achieved using a 1,2-diaminoethane linker, which presented in target **3** the same number of linking atoms from the (i + 2) Asn residue as provided by the propylamino linker in parent **2**.

* Corresponding author. Tel.: +1 301 846 5906; fax: +1 301 846 6033; e-mail: tburke@helix.nih.gov

0960-894X/$ - see front matter © 2005 Elsevier Ltd. All rights reserved.
doi:10.1016/j.bmcl.2005.01.017

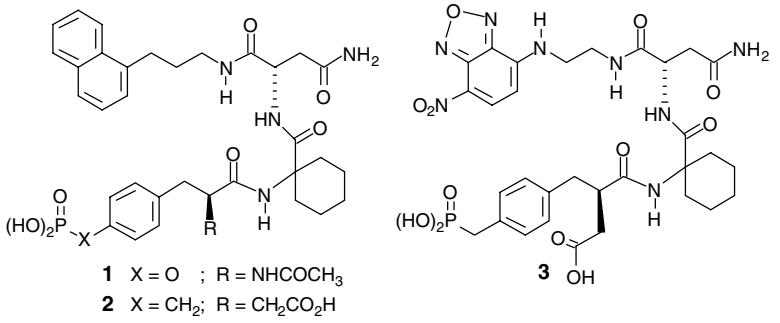

Figure 1. Structures of parent compounds **1** and **2** and the target fluorescent ligand **3**.

Accordingly, **4** was obtained by reaction of commercially-available 4-chloro-7-nitrobenzofurazane with ethylenediamine as previously reported (Scheme 1).[6] Coupling of **4** with N^{α}-Boc-Asn-OH in the presence of 1-hydroxybenzotriazole (HOBt) and diisopropylcarbodiimide (DIPCDI) provided **5** (72% yield),[7] which upon Boc-deprotection using TFA gave **6** (84% yield).[8] HOBt mixed anhydride coupling of **6** with commercially available N^{α}-Fmoc 1-aminocyclohexanecarboxylic acid (N^{α}-Fmoc Ac_6c) gave **7** (78% yield),[9] which was treated with piperidine to yield the N^{α}-deprotected **8** (79% yield).[10] The next step required coupling of **8** with the known pTyr mimetic **9**.[2c] This proved troublesome, possibly due to steric hindrance between the Ac_6c ring and the bulky α-($CH_2CO_2{}^tBu$) group. However, application of active ester coupling using 1-hydroxy-7-azabenzotriazole (HOAt) and 1-ethyl-3-(3′-dimethylamino)propyl)carbodiimide (EDCI)) at elevated temperature (50 °C) produced **10** in 37% yield.[11] Global removal of Bu^t-ester protecting groups by treatment with TFA in the presence of 1,2-ethanedithiol followed by HPLC purification provided target **3** as an orange amorphous powder.[12] For binding analysis, **3** was converted to its tri-sodium salt **3s** by treatment with $NaHCO_3$.

2. Determination of Grb2 SH2 domain-binding affinity

Binding affinity of **3s** as determined using an ELISA-based competition assay[13] provided an IC_{50} value of 167 nM ± 44 nM. Complimentary analysis using surface plasmon resonance (SPR) that measured the direct binding of **3s** to chip-bound Grb2 SH2 domain protein was conducted using a Biacore S51 instrument with biotinylated protein attached to neutravidin chips (Fig. 2).[14] In reasonable agreement with the ELISA results, a K_D value of 119 nM ± 0.6 nM was obtained, with kinetic parameters being $k_{on} = 1.18 \times 10^6 \pm 4.6 \times 10^3\ M^{-1}\,s^{-1}$ and $k_{off} = 1.40 \times 10^{-1} \pm 4.5 \times 10^{-4}\ s^{-1}$. This can be contrasted to SPR data recently reported for the parent analogue **2**, where a K_D value of 23.8 nM ± 1.8 nM was obtained, with kinetic parameters being k_{on} =

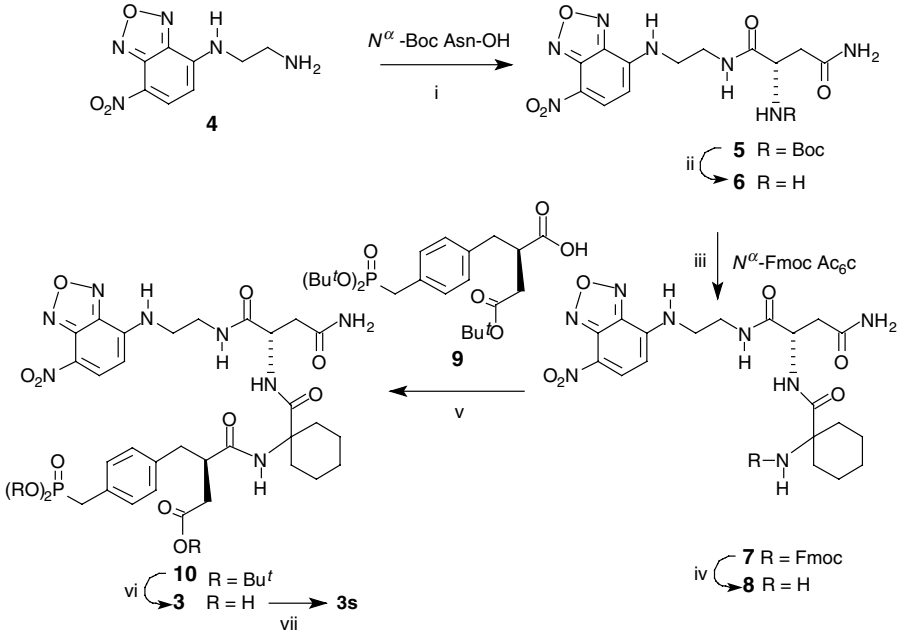

Scheme 1. Reagents and conditions: (i) DIPCDI, HOBt, DMF, rt, overnight (72% yield); (ii) TFA, CH_2Cl_2 1 h (84% yield); (iii) HOBt, DIPCDI, DMF, rt, overnight (78% yield); (iv) piperidine, CH_3CN, rt, 1 h (79% yield); (v) EDCI·HCl, HOAt, DMF, 50 °C, 24 h (37% yield); (vi) TFA, $HS(CH_2)_2SH$, H_2O, rt, 1 h (42% yield); (vii) $NaHCO_{3(aq)}$ (quantitative).

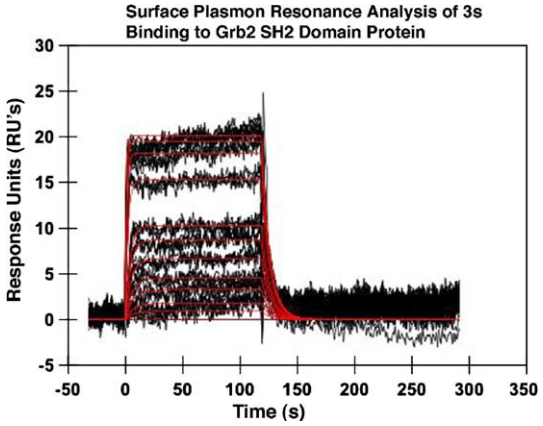

Figure 2. Using a Biacore S51 instrument, a series of 5, 10, 20, 30, 50, 75, 100, 250, 500, 750, and 1000 nM injections of **3s** were passed at a flow rate of 30 $\mu L\,min^{-1}$ over a neutravidin chip containing 8024 RU's of biotinylated Grb2 SH2 domain protein. Data represents the results of two duplicate injections, with mathematical fitting to a one component binding model indicated in red.

$4.18 \times 10^6 \pm 2.88 \times 10^3\ M^{-1}\,s^{-1}$ and $k_{off} = 9.91 \times 10^{-2} \pm 2.94 \times 10^{-3}\ s^{-1}$.[14] The 5-fold loss of binding affinity incurred by replacement of the 1-naphthyl ring system by the NBD ring system was due primarily to a 3.5-fold reduction in on-rate, with less effect arising from the off-rate (1.4-fold increase).

3. Modeling studies

To compare the hypothetical binding modes of **2** and **3**, molecular dynamics simulations were performed on pre-minimized protein–ligand complexes using Macromodel 8.6.[15] Chain A from the crystal structure of mAZ-pY-(αMe)pY-N-NH_2 bound to the Grb2 SH2 domain (1JYQ.pdb)[16] was used as the starting geometry for the modeling study. All minimizations and simulations were performed using the Merck Molecular Force Field (MMFFs)[17] and a continuum solvation model for H_2O (GB/SA).[18] Both compounds exhibited all binding interactions that have previously been shown by X-ray crystallography to be important for this class of compound. However, two major differences were observed between **2** and **3**. First, the α-CH_2COOH of **3** was H-bonded to GlnβD3 (Gln106), while the same group did not exhibit any H-bonding interactions in **2**. Although this additional H-bonding interaction should have favored the binding of **3** as compared to **2**, interactions of the C-terminal NBD moiety of **3** were not as favorable as for the naphthyl group of **2**. While the C-terminal naphthylpropyl portion of **2** made van der Waals interactions with a hydrophobic region defined by residues LeuβD8 and PheβE3, the NMD group of **3** was found to occupy a site closer to a hydrophilic region on the surface of the Grb2 SH2 domain, and even here significant binding interactions were not noted (Fig. 3).

In order to further understand the binding modes of **2** and **3**, the electrostatic potential on the solvent-accessible surface of the Grb2 SH2 domain protein as well as for compounds **2** and **3** were calculated using the Delphi module in the Insight II program.[19] The default Delphi formal charges were applied for the protein, while for **2** and **3** charges were obtained using ab initio calculations with Gaussian 03[20] (results not shown). It was observed that the electrostatic potential of the 2-naphthyl ring system of **2** was complementary to the protein surface potential proximal to it, thereby promoting binding interactions. In contrast, the electrostatic potentials on the NBD moiety of **3** and on the hydrophilic protein surface proximal to it were both electronegative, thus promoting less favorable interactions. The noncomplementary electrostatic potentials observed between the NBD group of **3** and Grb2 SH2 domain protein may contribute to its reduced binding affinity relative to **2**.

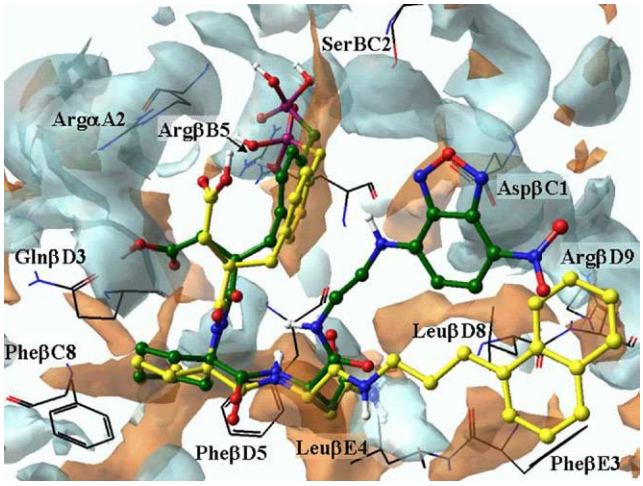

Figure 3. Hypothetical Grb2 SH2 domain binding modes of **2** and **3**. Coloring of atoms is: carbon—yellow (for **2**) or dark green (for **3**); nitrogen—blue; oxygen—red; hydrogen—white. Hydrophilic and hydrophobic surface maps are colored in turquoise and orange, respectively, with certain key residues closest to the surface maps being displayed in wire representation.

In summary, title compound **3** represents a low nanomolar affinity Grb2 SH2 domain-binding inhibitor that utilizes the environmentally-sensitive NBD fluorophore. Although modeling studies suggest that the level of bonding interactions afforded by the NBD ring system may not be as great as those provided by the naphthyl ring, which it replaces, this novel agent should serve as a useful tool to investigate the actions of this class of Grb2 SH2 domain-binding antagonists in whole cell systems.

Acknowledgements

Appreciation is expressed to Drs. Christopher Lai and James Kelley of the LMC for mass spectral anaysis.

References and notes

1. (a) Daly, R. J.; Binder, M. D.; Sutherland, R. L. *Oncogene* **1994**, *9*, 2723; (b) Garbay, C.; Liu, W. Q.; Vidal, M.; Rogues, B. P. *Biochem. Pharmacol.* **2000**, *60*, 1165; (c) Dankort, D.; Maslikowski, B.; Warner, N.; Kanno, N.;

Kim, H.; Wang, Z. X.; Moran, M. F.; Oshima, R. G.; Cardiff, R. D.; Muller, W. J. *Mol. Cell. Biol.* **2001**, *21*, 1540; (d) Saucier, C.; Papavasiliou, V.; Palazzo, A.; Naujokas, M. A.; Kremer, R.; Park, M. *Oncogene* **2002**, *21*, 1800; (e) Osada, S.; Saji, S. *Curr. Med. Chem., Anti-Cancer Agent* **2003**, *3*, 119; (f) Feller, S. M.; Tuchscherer, G.; Voss, J. *Leukemia Lymphoma* **2003**, *44*, 411.

2. (a) Furet, P.; Gay, B.; Caravatti, G.; Garcia-Echeverria, C.; Rahuel, J.; Schoepfer, J.; Fretz, H. *J. Med. Chem.* **1998**, *41*, 3442; (b) Yao, Z. J.; King, C. R.; Cao, T.; Kelley, J.; Milne, G. W. A.; Voigt, J. H.; Burke, T. R. *J. Med. Chem.* **1999**, *42*, 25; (c) Wei, C.-Q.; Li, B.; Guo, R.; Yang, D., Jr.; Burke, T. R., Jr. *Bioorg. Med. Chem. Lett.* **2002**, *12*, 2781.
3. Numerous reports have appeared detailing the use of fluorescent ligands to study protein interactions within cellular contexts. For recent examples, see: (a) Berque-Bestel, I.; Soulier, J.-L.; Giner, M.; Rivail, L.; Langlois, M.; Sicsic, S. *J. Med. Chem.* **2003**, *46*, 2606; (b) Ettmayer, P.; Billich, A.; Baumruker, T.; Mechtcheriakova, D.; Schmid, H.; Nussbaumer, P. *Bioorg. Med. Chem. Lett.* **2004**, *14*, 1555.
4. Nomenclature as suggested by Eck et al. *Nature* **1994**, *362*, 87.
5. Schoepfer, J.; Fretz, H.; Gay, B.; Furet, P.; Garcia-Echeverria, C.; End, N.; Caravatti, G. *Bioorg. Med. Chem. Lett.* **1999**, *9*, 221.
6. Cotte, A.; Bader, B.; Kuhlmann, J.; Waldmann, H. *Chem. Eur. J.* **1999**, *5*, 922.
7. *Compound* **5**: H NMR (d_6-DMSO) δ 9.18 (m, 1H), 8.53 (d, 1H, J = 8.9 Hz), 7.73–7.70 (m, 2H), 7.25 (s, 1H), 6.86 (s, 1H), 6.45 (d, 1H, J = 9.1 Hz), 4.15 (m, 1H), 3.53–3.50 (m, 2H), 3.46–3.41 (m, 2H), 2.42 (dd, 1H, J = 5.5 Hz & 15.1 Hz), 2.34 (m, 1H), 1.38 (s, 9H). FABMS (+Ve) *m/z* 438 [MH^+].
8. *Compound* **6**: H NMR (d_6-DMSO) δ 8.84 (m, 1H), 8.54 (d, 1H, J = 8.5 Hz), 7.90 (m, 1H), 7.67 (m, 1H), 7.45 (m, 1H), 7.20 (s, 1H), 6.50 (d, 1H, J = 8.6 Hz), 4.01 (m, 1H), 3.64–3.47 (m, 4H), 2.73 (dd, 1H, J = 5.0 Hz & 15.3 Hz), 2.63 (dd, 1H, J = 7.8 Hz & 15.4 Hz). FABMS (+Ve) *m/z* 338 [MH^+].
9. *Compound* **7**: H NMR ($CDCl_3$) δ 8.13 (d, 1H, J = 8.6 Hz), 7.98 (d, 1H, J = 8.6 Hz), 7.77 (m, 1H), 7.64 (dd, 2H, J = 0.6 Hz & 7.6 Hz), 7.43 (dd, 2H, J = 1.0 Hz & 7.6 Hz), 7.33–7.29 (m, 3H), 7.22–7.18 (m, 3H), 5.84 (s, 1H), 5.79 (d, 1H, J = 8.4 Hz), 5.38 (s, 1H), 4.68 (m, 1H), 4.26 (dd, 1H, J = 7.0 Hz & 10.5 Hz), 4.20 (dd, 1H, J = 7.2 Hz & 10.5 Hz), 4.08 (m, 1H), 3.56 (m, 1H), 3.42–3.31 (m, 2H), 3.24 (m, 1H), 3.08 (dd, 1H, J = 4.4 Hz & 15.7 Hz), 2.40 (dd, 1H, J = 4.5 Hz & 15.6 Hz), 2.09–1.18 (m, 10H). FABMS (+Ve) *m/z* 685 [MH^+].
10. *Compound* **8**: H NMR (CD_3OD) δ 8.36 (d, 1H, J = 8.8 Hz), 6.32 (d, 1H, J = 8.9 Hz), 4.67 (m, 1H), 3.68–3.53 (m, 4H), 2.78 (dd, 1H, J = 6.7 Hz & 15.4 Hz), 2.72 (dd, 1H, J = 5.9 Hz & 15.5 Hz), 1.93–1.30 (m, 10H). FABMS (+Ve) *m/z* 463 [MH^+].
11. *Compound* **10**: H NMR ($CDCl_3$) δ 8.34 (d, 1H, J = 8.6 Hz), 7.98 (s, 1H), 7.88 (s, 1H), 7.81 (d, 1H, J = 7.9 Hz), 7.15 (dd, 2H, J = 2.4 Hz & 8.1 Hz), 7.03 (d, 2H, J = 7.9 Hz), 6.98 (s, 1H), 6.66 (s, 1H), 6.12 (d, 1H, J = 8.2 Hz), 5.73 (s, 1H), 4.56 (m, 1H), 3.77 (m, 1H), 3.64 (s, 1H), 3.48 (m, 1H), 2.97 (d, 2H, J = 21.4 Hz), 3.03–2.92 (m, 3H), 2.67 (dd, 1H, J = 4.4 Hz & 15.5 Hz), 2.57–2.50 (m, 2H), 2.32 (dd, 1H, J = 2.7 Hz & 17.6 Hz), 1.97 (m, 1H), 1.85–1.15 (m, 10H), 1.40 (s, 9H), 1.39 (s, 9H), 1.37 (s, 9H). FABMS (+Ve) *m/z* 915 [MH^+].
12. *Compound* **3**: H NMR (d_6-DMSO) δ 9.38 (t, 1H, J = 6.0 Hz), 8.51 (d, 1H, J = 9.0 Hz), 8.29 (s, 1H), 7.70–7.66 (m, 2H), 7.35 (s, 1H), 7.16–7.09 (m, 4H), 6.89 (s, 1H), 6.44 (d, 1H, J = 9.0 Hz), 4.33 (m, 1H), 3.58–3.52 (m, 2H), 3.41–3.37 (m, 2H), 3.10 (m, 1H), 2.97 (dd, 1H, J = 5.0 Hz & 13.3 Hz), 2.89 (d, 2H, J = 21.3 Hz), 2.62 (dd, 1H, J = 6.6 Hz & 15.6 Hz), 2.50 (dd, 1H, J = 5.1 Hz & 15.5 Hz), 2.43 (dd, 1H, J = 10.4 Hz & 16.9 Hz), 2.32 (dd, 1H, J = 9.9 Hz & 13.1 Hz), 1.98 (dd, 1H, J = 4.1 Hz & 16.8 Hz), 1.84–1.07 (m, 10H). FABMS (+Ve) *m/z* 745 [M−H].
13. *ELISA procedure*: Streptavidin-coated 96 well plates were first blocked with 0.2% I-Block (Tropix Applied Biosystems, Bedford, MA). A recombinant chimeric protein encompassing the human Grb2 SH2 domain sequence (residues 60–151, accession number P29354) fused in frame with the complete maltose binding protein sequence and a carboxyl terminal 6-histidine tag was expressed in *E. coli*, biotinylated, and purified by conventional methods. Approximately 1 mg/mL of protein solution was diluted to 10 μg/mL in 0.1% BSA/TPBS before adding to appropriate wells (100 μL/well). Plates were then incubated at RT for 2 h followed by three washes with TPBS. To each well was added human epidermal growth factor receptor-derived Grb2 SH2 domain recognition sequence (NH_2-biotin-DDTFLPVPE-pYINQSVPK-COOH) conjugated to horse radish peroxidase (HRP, 100 μL at 20 μg/mL) in the presence or absence of varying concentrations of **3s**, then the plates were incubated for 1 h at rt. Following incubation, plates were washed with TPBS, then to each well was added TPBS (50 μL) and ELISA detection reagent OPD (50 μL; Abbott Laboratories Diagnostic Division, Abbott Park, IL; Cat # 0617230). Absorbance was measured in an ELISA plate reader at 450 nm. A minimum of four replicate wells was analyzed for each antagonist concentration. Regression analysis, IC_{50} values, and statistically significant differences were determined using GraphPad InStat Software analysis of two or more independent ELISA experiments.
14. Oishi, S.; Karki, R. G.; Kang, S.-U.; Wang, X.; Worthy, K. M.; Bindu, L. K.; Nicklaus, M. C.; Fisher, R. J.; Burke, T. R., Jr. *J. Med. Chem.*, in press.
15. Mohamadi, F.; Richards, N. G. J.; Guida, W. C.; Liskamp, R.; Lipton, M.; Caufield, C.; Chang, G.; Hendrickson, T.; Still, W. C. *J. Comput. Chem.* **1990**, *11*, 440.
16. Nioche, P.; Liu, W. Q.; Broutin, I.; Charbonnier, F.; Latreille, M. T.; Vidal, M.; Roques, B.; Garbay, C.; Ducruix, A. *J. Mol. Biol.* **2002**, *315*, 1167.
17. Halgren, T. A. *J. Comput. Chem.* **1996**, *17*, 490.
18. Qiu, D.; Shenkin, P. S.; Hollinger, F. P.; Still, W. C. *J. Phys. Chem. A* **1997**, *101*, 3005.
19. Computational results were obtained using the software program Insight II by Accelrys Inc., San Diego, CA (http://www.accelrys.com/).
20. Frisch, M. J.; et al. Gaussian 03, Revision B.04 2003.